Molecular Systems Biology 5; Article number 280; doi:10.1038/msb.2009.39
Citation: ***Molecular Systems Biology*** **5:280**

www.molecularsystemsbiology.com

molecular systems biology

Prediction and validation of a mechanism to control the threshold for inhibitory synaptic plasticity

Yuichi Kitagawa[1,2], Tomoo Hirano[1,2] and Shin-ya Kawaguchi[1,2,*]

[1] Department of Biophysics, Graduate School of Science, Kyoto University, Sakyo-ku, Kyoto, Japan and [2] CREST, Japan Science and Technology Agency, Kawaguchi, Saitama, Japan
* Corresponding author. Department of Biophysics, Graduate School of Science, Kyoto University, Oiwake-cho, Sakyo-ku, Kyoto 606-8502, Japan.
Tel.: +81 75 753 4238; Fax: +81 75 753 4229; E-mail: kawaguchi@neurosci.biophys.kyoto-u.ac.jp

Received 29.12.08; accepted 14.5.09

Synaptic plasticity, neuronal activity-dependent sustained alteration of the efficacy of synaptic transmission, underlies learning and memory. Activation of positive-feedback signaling pathways by an increase in intracellular Ca^{2+} concentration ($[Ca^{2+}]_i$) has been implicated in synaptic plasticity. However, the mechanism that determines the $[Ca^{2+}]_i$ threshold for inducing synaptic plasticity is elusive. Here, we developed a kinetic simulation model of inhibitory synaptic plasticity in the cerebellum, and systematically analyzed the behavior of intricate molecular networks composed of protein kinases, phosphatases, etc. The simulation showed that Ca^{2+}/calmodulin-dependent protein kinase II (CaMKII), which is essential for the induction of synaptic plasticity, was persistently activated or suppressed in response to different combinations of stimuli. The sustained CaMKII activation depended on synergistic actions of two positive-feedback reactions, CaMKII autophosphorylation and CaMKII-mediated inhibition of a CaM-dependent phosphodiesterase, PDE1. The simulation predicted that PDE1-mediated feedforward inhibition of CaMKII predominantly controls the Ca^{2+} threshold, which was confirmed by electrophysiological experiments in primary cerebellar cultures. Thus, combined application of simulation and experiments revealed that the Ca^{2+} threshold for the cerebellar inhibitory synaptic plasticity is primarily determined by PDE1.
Molecular Systems Biology 5: 280; published online 16 June 2009; doi:10.1038/msb.2009.39
Subject Categories: neuroscience; signal transduction
Keywords: Ca^{2+} threshold; computer simulation; PDE1; Purkinje neuron; synaptic plasticity

Introduction

Interactions of intracellular signaling pathways including feedforward and feedback loops underlie various cellular behaviors such as oscillations, adaptations, bistability, and/or robustness (Brandman and Meyer, 2008). One bistable phenomenon depending on feedback signaling pathways is the neuronal activity-dependent synaptic plasticity, that is, sustained alteration of information transmission efficacy between neurons. Many forms of synaptic plasticity have been reported at both excitatory and inhibitory synapses in various regions of the central nervous system and have been regarded as cellular bases for learning and memory (Kano *et al*, 1992; Komatsu, 1996; Nusser *et al*, 1998; Bailey *et al*, 2000; Hansel *et al*, 2001; Ito, 2001; Kandel, 2001; Gaiarsa *et al*, 2002). In most cases, synaptic plasticity is induced by an increase in intracellular Ca^{2+} concentration ($[Ca^{2+}]_i$) and regulated by complex downstream molecular networks consisting of numerous molecules such as protein kinases and phosphatases (Malenka and Nicoll, 1999; Lisman *et al*, 2002; Sheng and Kim, 2002). Thus, it is difficult to comprehend quantitatively how the whole molecular network regulates the synaptic plasticity in response to a $[Ca^{2+}]_i$ increase. To overcome this difficulty, computational models have been developed to simulate the molecular networks regulating synaptic plasticity such as hippocampal long-term potentiation (LTP), cerebellar long-term depression (LTD), and long-term facilitation in *Aplysia* (Bhalla and Iyengar, 1999; Kuroda *et al*, 2001; Doi *et al*, 2005; Pettigrew *et al*, 2005). These simulations have shown that activation of a positive-feedback loop inherent in the molecular network has an important function in the establishment of synaptic plasticity.

At GABAergic synapses on cerebellar Purkinje neurons, postsynaptic depolarization such as that caused by inputs from a climbing fiber induces LTP of postsynaptic $GABA_A$ receptor ($GABA_AR$) responsiveness, which is called rebound potentiation

(RP) (Kano *et al*, 1992). Induction of RP requires a postsynaptic $[Ca^{2+}]_i$ increase and the subsequent activation of Ca^{2+}/calmodulin (CaM)-dependent protein kinase II (CaMKII) (Kano *et al*, 1992, 1996). We reported earlier that the activation of presynaptic interneurons during postsynaptic depolarization suppresses RP through activation of postsynaptic metabotropic $GABA_B$ receptors ($GABA_BRs$) (Kawaguchi and Hirano, 2000). The suppressive effect of $GABA_BR$ is mediated by downregulation of PKA (protein kinase A) through inhibition of adenylyl cyclase. Reduction of PKA activity facilitates calcineurin (a Ca^{2+}-activated protein phosphatase, also called PP2B)-mediated dephosphorylation of DARPP-32 (dopamine and cAMP-regulated phosphoprotein, 32 kDa) (Kawaguchi and Hirano, 2002). As DARPP-32 phosphorylated by PKA inhibits protein phosphatase 1 (PP-1), reduction of PKA activity by $GABA_BR$ would release PP-1 from the inhibition. As a result, $GABA_BR$ activation is thought to counteract CaMKII activity and suppress RP induction (Kawaguchi and Hirano, 2000, 2002). However, it is enigmatic how the overall signaling pathways inferred from combining fragmentary experimental results operate to determine whether RP is induced or not in response to various patterns of inputs. To address this issue, we developed a kinetic simulation model of the molecular network and systematically analyzed the behavior of signaling cascades regulating RP. Our simulation reproduced the RP induction and its suppression in response to different combinations of inputs, and suggested the important role of cooperative actions of two positive-feedback loops, CaMKII autophosphorylation and CaMKII-mediated downregulation of phosphodiesterase 1 (PDE1), a type of Ca^{2+}/CaM-dependent PDE. It also predicted that feedforward inhibition of CaMKII by a pathway including PDE1 predominantly determined the Ca^{2+} threshold for RP induction, which was confirmed by electrophysiological experiments.

Results

Signaling pathways in the simulation model

A kinetic simulation model of signaling cascades regulating RP was constructed based on our earlier study (Kawaguchi and Hirano, 2002) with slight modification (Figure 1A). RP is induced by a $[Ca^{2+}]_i$ increase and the resultant CaMKII activation (Kano *et al*, 1992, 1996). Both α- and β-isoforms of CaMKII were expressed in Purkinje neurons (Supplementary Figure 1). As described in Supplementary information, we assumed here that the same amounts of α and β CaMKII exist in Purkinje neurons. For effective activation of CaMKII, the activity of PP-1 should be inhibited by DARPP-32 that has been phosphorylated by PKA. Ca^{2+}/CaM-activated calcineurin increases the PP-1 activity through dephosphorylation of DARPP-32, counteracting the CaMKII activity (Figure 1A). Thus, regulation of DARPP-32 phosphorylation by PKA has an important function in the switching of whether RP is induced or not (Kawaguchi and Hirano, 2002). It was suggested that $GABA_BR$ suppresses the RP induction by reducing the amount of cAMP and the PKA activity by G_i-mediated inhibition of adenylyl cyclase (Kawaguchi and Hirano, 2000).

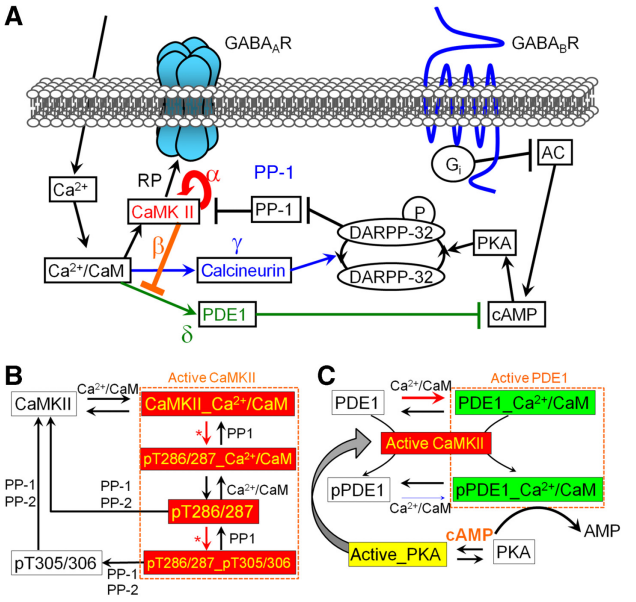

Figure 1 Signaling cascades of the RP regulation. (**A**) Pathway diagram of the signaling cascades. There are two positive-feedback pathways (α, β) and two feedforward inhibitory pathways for CaMKII activation (γ, δ). (**B**) Schematic representation of positive-feedback system of CaMKII (marked 'α' in A). After activation by Ca^{2+}/CaM binding, CaMKII autophosphorylates Thr286/287 and Thr305/306 (marked by *). Phosphorylation of Thr286/287 maintains the enzymatic activity without Ca^{2+}/CaM. (**C**) Phosphorylation of PDE1 by CaMKII forms a positive-feedback loop (marked 'β' in A). CaMKII-mediated phosphorylation of PDE1 reduces the affinity to Ca^{2+}/CaM. As a result, PDE activity is reduced, leading to augmentation of PKA activity. As PKA activity indirectly supports CaMKII activity, reduced PDE1 activity contributes to CaMKII activation.

Feedforward and feedback loops in a network contribute to the nonlinear performance of the system, and there are such loops in the signaling cascades regulating the RP induction. Calcineurin-mediated DARPP-32 dephosphorylation and PP-1 activation is a feedforward inhibitory pathway to CaMKII activation. One positive-feedback loop is autophosphorylation at Thr286 of α-CaMKII and Thr287 of β-CaMKII (Figure 1A and B). When Thr286/287 is phosphorylated, CaMKII maintains its enzymatic activity in the absence of Ca^{2+}/CaM (Miller and Kennedy, 1986; Lisman *et al*, 2002), which would contribute to the maintenance of long-lasting potentiation of synaptic transmission.

To incorporate the cAMP regulation, here we have added PDE1 and PDE4 (both of which are expressed in Purkinje neurons, see Supplementary Figure 1) to the simulation model. PDE1 is activated by Ca^{2+}/CaM to hydrolyze cAMP and cGMP, whereas PDE4 is Ca^{2+}/CaM-independent and cAMP specific (Polli and Kincaid, 1994; Yu *et al*, 1997; Cherry and Davis, 1999). Taking into consideration the fact that the PKA activity is required for effective CaMKII activation, it seems that Ca^{2+}-dependent PDE1 activation functions as another feedforward inhibitory pathway to CaMKII (Figure 1A). Interestingly, the affinity of B-type of PDE1 (PDE1B) for Ca^{2+}/CaM is reduced when it is phosphorylated by CaMKII (Hashimoto *et al*, 1989). As shown in Supplementary Figure 1, PDE1B was highly expressed in Purkinje neurons (Polli and Kincaid, 1994; Yu *et al*, 1997). Thus, we assumed that PDE1 is negatively regulated by CaMKII in the model. The

increase in cAMP concentration caused by PDE1 inhibition would lead to the increased PKA activity, which would in turn support the CaMKII activity through facilitating the inhibition of PP-1 by phospho-DARPP-32. Thus, CaMKII-mediated inhibition of PDE1 might work as a positive-feedback loop (Figure 1A and C). Altogether, the kinetic simulation model for the RP regulation includes two feedforward inhibitory pathways (PDE1 and calcineurin pathways) and two positive-feedback loops (autophosphorylation of CaMKII Thr286/287 and inhibition of PDE1 by CaMKII). CaMKII can directly phosphorylate the $GABA_AR$ β and γ subunits, which positively regulates the receptor responsiveness (Houston and Smart, 2006). Thus, we analyzed the CaMKII activity and the phosphorylation level of $GABA_AR$s with the model.

Sustained CaMKII activation or its suppression by different combinations of Ca^{2+} and GABA stimulation

Using the simulation model, we first attempted to reproduce the earlier experimental findings that different combinations of $[Ca^{2+}]_i$ increase and $GABA_BR$ activation result in RP induction or suppression. The basal level of $[Ca^{2+}]_i$ and the extracellular GABA concentration were set at 0.1 and 0.01 μM, respectively. When $[Ca^{2+}]_i$ was increased to 1 μM for 10 s, the amount of active CaMKII was increased for a long time (Figure 2A, red line). Without the Ca^{2+} stimulus, it stayed low (data not shown). Thus, the total CaMKII activity shifted from a low level (∼0.001 μM) to a high level (∼5 μM) after a transient $[Ca^{2+}]_i$ increase. As a result, phosphorylated $GABA_AR$ increased persistently (Figure 2B). In response to the transient $[Ca^{2+}]_i$ increase, the amount of Ca^{2+}/CaM complex increased rapidly and then decreased to the basal level (Figure 2C). Accordingly, both calcineurin and PDE1 were activated by the $[Ca^{2+}]_i$ increase (Figure 2D and E). After the end of the $[Ca^{2+}]_i$ increase, the amount of active calcineurin rapidly returned to the basal level, whereas that of active PDE1 showed a sustained decrease (Figure 2D and E). This sustained decrease of PDE1 activity was caused by CaMKII-mediated reduction of the affinity of PDE1 for Ca^{2+}/CaM, as described below. Thus, the amounts of cAMP and active PKA were transiently decreased by PDE1 activation during the $[Ca^{2+}]_i$ increase, and then showed a sustained increase after the end of the $[Ca^{2+}]_i$ increase (Figure 2G and H). As a result, the phosphorylation level of DARPP-32 also exhibited a transient decrease, followed by a sustained increase (Figure 2I). Therefore, the amount of active PP-1 transiently increased in response to the $[Ca^{2+}]_i$ increase and subsequently showed a long-term decrease (Figure 2J). In summary, sustained CaMKII activation and $GABA_AR$ phosphorylation were accompanied by long-term decreases in the amounts of active PP-1 and PDE1 (Figure 2E and J), and by sustained increases in the amounts of phospho-DARPP-32, cAMP, and active PKA (Figure 2A, B, and G–I). On the other hand, the amounts of active Ca^{2+}/CaM, calcineurin, and adenylyl cyclase after the Ca^{2+} stimulation returned to their respective basal levels (Figure 2C, D and F).

We next examined the effect of $GABA_BR$ activation coupled with a $[Ca^{2+}]_i$ increase. When GABA concentration was increased to 50 μM during the 10-s $[Ca^{2+}]_i$ increase, the total CaMKII activity and $GABA_AR$ phosphorylation rapidly returned to the basal levels after the conditioning stimulation (Figure 2A and B, blue lines). Compared with the results without $GABA_BR$ stimulation, the reductions of the cAMP and active PKA levels during the conditioning stimulation were larger (Figure 2G and H), and the duration of the increase in active PP-1 was longer (Figure 2J). Thus, $GABA_BR$ activation suppressed the sustained CaMKII activation, as suggested by our earlier experiments (Kawaguchi and Hirano, 2002). Taken together, these results indicate that a $[Ca^{2+}]_i$ increase alone or coupled with $GABA_BR$ activation caused a sustained increase in active CaMKII or its suppression, respectively, which would correspond to whether RP was induced or not.

We next examined whether the bistable behavior of the signaling cascades, which is reflected by the high and low levels of CaMKII activity in response to a $[Ca^{2+}]_i$ increase with or without concurrent $GABA_BR$ activation, depends on the basal $[Ca^{2+}]_i$ and/or the intensity or duration of each stimulation. At any value of basal $[Ca^{2+}]_i$ between 50 and 110 nM, the CaMKII activity at 30 min after the $[Ca^{2+}]_i$ increase was higher than that after the coupled stimulation of a $[Ca^{2+}]_i$ increase and $GABA_BR$ activation (Figure 3A). It should be noted that the bistability of CaMKII activity was evident with a relatively high basal $[Ca^{2+}]_i$ (>0.093 μM), whereas with a lower basal $[Ca^{2+}]_i$, the CaMKII activity slowly decreased and finally returned to the basal level (Supplementary Figure 2). Thus, the CaMKII activation induced by a transient $[Ca^{2+}]_i$ increase did not necessarily continue forever. In any case, a transient $[Ca^{2+}]_i$ increase caused sustained CaMKII activation, which was largely suppressed by simultaneous $GABA_BR$ activation.

When the duration of conditioning stimulation was shorter, a slightly larger $[Ca^{2+}]_i$ increase was required for triggering sustained CaMKII activation (0.6 μM for 10 s; 0.7 μM for 5 s; 1.1 μM for 1 s; 1.5 μM for 0.5 s) (Figure 3B–E). On the other hand, shortening the duration of coupled conditioning stimulation consisting of $GABA_BR$ activation and the $[Ca^{2+}]_i$ increase dramatically weakened the suppressive effect of $GABA_BR$ activation on the CaMKII activation (Figure 3B–E; also see Supplementary Figure 3). Thus, the induction of RP depends predominantly on the intensity rather than the duration of $[Ca^{2+}]_i$ increase, whereas its suppression depends more strongly on the duration than on the intensity of $GABA_BR$ activation. These properties of the signaling networks were also evident with a lower basal $[Ca^{2+}]_i$, with which the CaMKII activity finally returned to the basal level (data not shown).

Long-term activation of CaMKII in living Purkinje neurons

To test whether sustained activation of CaMKII takes place in living Purkinje neurons, we stained active CaMKII autophosphorylated at Thr286 (in the α subunit) or Thr287 (in the β subunit) after the transient $[Ca^{2+}]_i$ increase caused by depolarization. Cultured cerebellar neurons were depolarized for 10 s by treating with the external solution containing 50 mM K^+ and SCH50911 (10 μM, a selective antagonist for

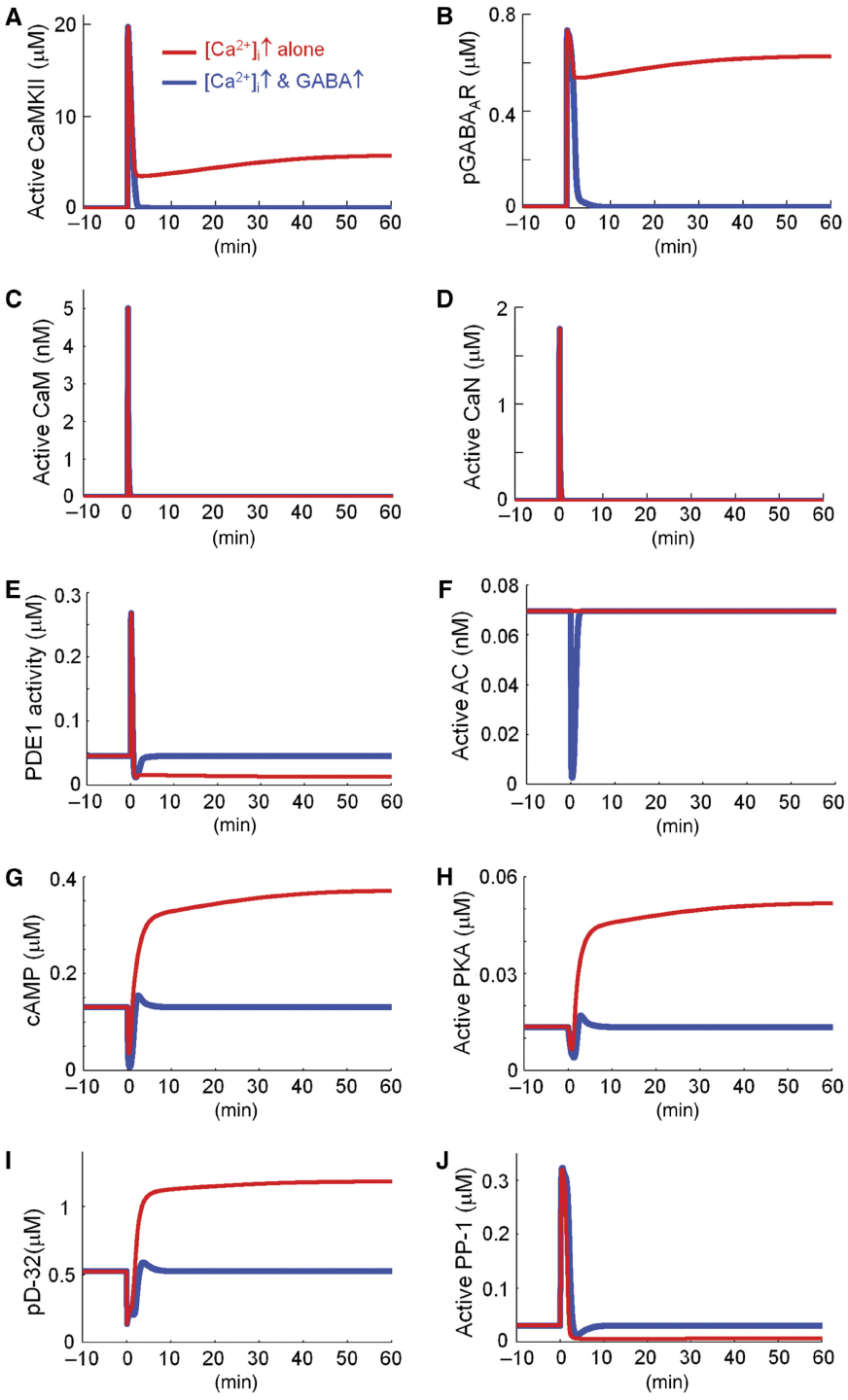

Figure 2 The changes of amount of molecules in signaling cascades induced by a $[Ca^{2+}]_i$ increase with or without concurrent $GABA_BR$ activation. Simulated time courses of the amount of active CaMKII (**A**), phosphorylated $GABA_AR$ (**B**), Ca^{2+}/CaM (**C**), active calcineurin (CaN) (**D**), active PDE1 (**E**), active adenylyl cyclase (AC) (**F**), cAMP (**G**), active PKA (**H**), phosphorylated DARPP-32 (pD-32) (**I**), and active PP-1 (**J**) in response to the conditioning stimuli (at 0 min for 10 s) consisting of either a $[Ca^{2+}]_i$ increase alone (1 μM, red line) or a $[Ca^{2+}]_i$ increase plus a GABA increase (50 μM, blue line).

$GABA_BRs$), which was added to avoid activation of $GABA_BRs$ by GABA released from depolarized presynaptic terminals of inhibitory neurons. The fluorescent signal of active CaMKII increased for >2 h after the conditioning K^+ treatment (247 ± 14% at 0.5 h; 198 ± 14% at 2 h), whereas it was not significantly elevated at 5 h (101 ± 9% at 5 h) (Figure 4A and B). In contrast, when $GABA_BRs$ were activated by baclofen (a selective agonist of $GABA_BRs$, 50 μM) during the K^+-mediated depolarization, the sustained CaMKII activation was suppressed, as reported earlier (Kawaguchi and Hirano, 2002;

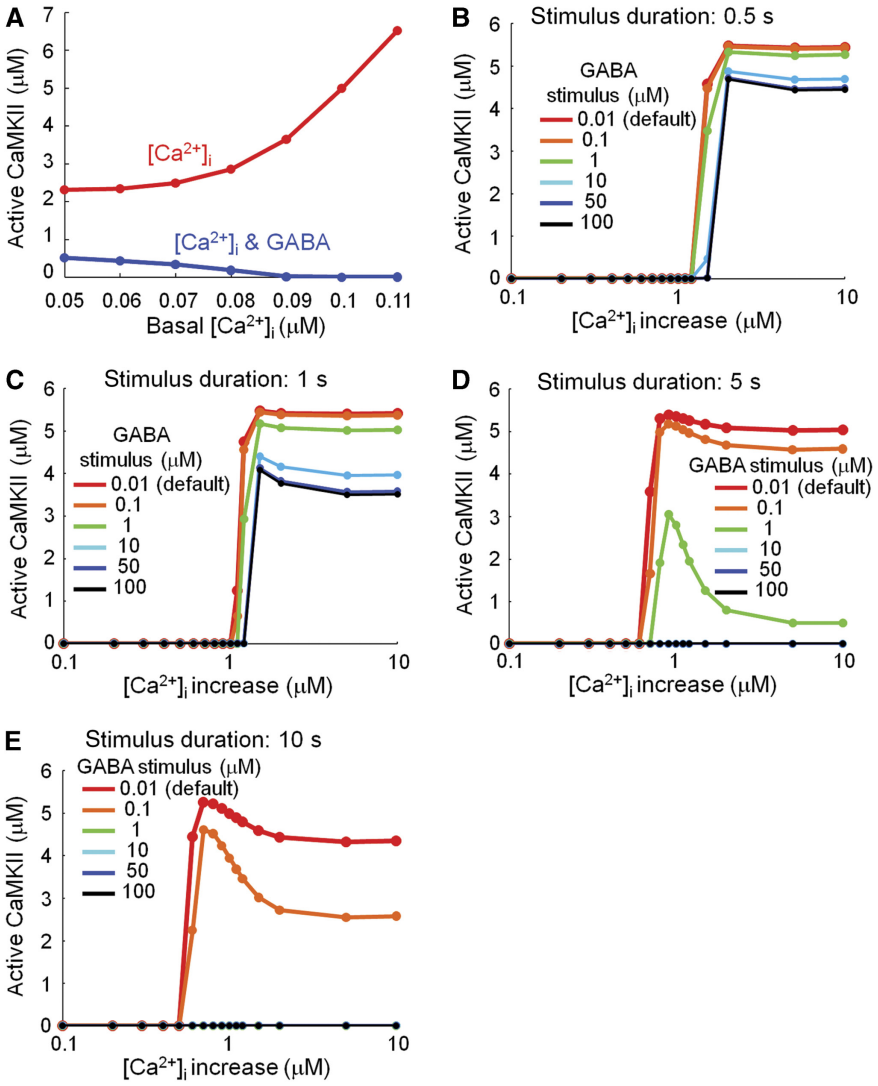

Figure 3 CaMKII activation under various conditions. (**A**) Effect of basal $[Ca^{2+}]_i$ on the amount of active CaMKII 30 min after the conditioning stimulation (a $[Ca^{2+}]_i$ increase (1 μM) either alone or coupled with a GABA increase (50 μM)). (**B**–**E**) The amount of active CaMKII at 30 min after the conditioning stimulation is plotted as a function of the amplitude of $[Ca^{2+}]_i$ increase. The amplitudes of GABA increase are represented by different colors. Durations of increase of $[Ca^{2+}]_i$ and GABA were 0.5 s (B), 1 s (C), 5 s (D), and 10 s (E). Source data is available for this figure at www.nature.com/msb.

Sugiyama *et al*, 2008) (data not shown). Thus, consistently with the simulation results, CaMKII was activated for a long time after brief depolarization of a Purkinje neuron, and this sustained activation was suppressed by $GABA_BR$ activation during the depolarization. Furthermore, application of a cell-permeable inhibitory peptide for CaMKII (Ant-AIP-II, 50 μM) at 30 min after the end of K^+ treatment, attenuated the sustained autophosphorylation at Thr286/287 (Figure 4C and D). Thus, the sustained increase in active CaMKII depends on the kinase activity of CaMKII, probably through some positive-feedback reaction. In addition, inhibition of Ca^{2+}/CaM binding to CaMKII by KN62 (5 μM), also abolished the maintenance of once-established phosphorylation at Thr286/287 (data not shown), suggesting that the CaMKII activity is likely sustained through dynamic equilibrium of phosphorylation of newly produced Ca^{2+}/CaM-bound CaMKII and dephosphorylation by phosphatases.

Synergistic action of CaMKII autophosphorylation and PDE1 inhibition by CaMKII

As discussed above, there are two positive-feedback reactions dependent on the CaMKII activity in the signaling networks. One is the autophosphorylation of CaMKII Thr286/287, which renders CaMKII Ca^{2+}-independently active (Miller and Kennedy, 1986; Lisman *et al*, 2002). The other is down-regulation of PDE1 by CaMKII through decreasing the affinity for Ca^{2+}/CaM (Hashimoto *et al*, 1989), which would facilitate the PP-1 inhibition by phospho-DARPP-32 through augmentation of the PKA activity. Thus, it is likely that CaMKII-mediated inhibition of PDE1 in turn supports the CaMKII activity. Using the simulation model, we tried to clarify whether each positive-feedback loop contributes to sustained CaMKII activation. When either phosphorylation was stopped by altering each k_{cat} to zero at 30 min after the transient $[Ca^{2+}]_i$

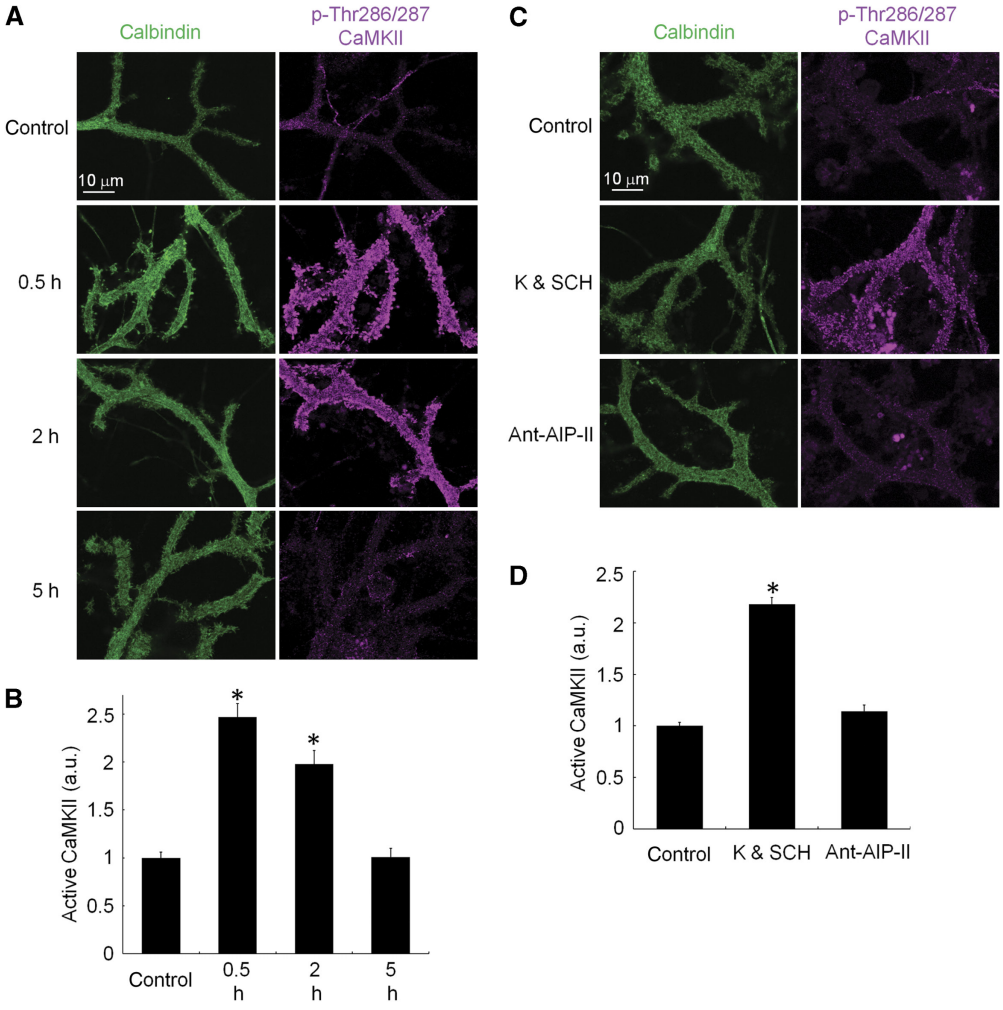

Figure 4 Sustained CaMKII activation in a living Purkinje neuron. (**A**) Immunofluorescent staining of phospho-Thr286/287 CaMKII (magenta) and calbindin (green) at the indicated times after the conditioning K^+ treatment for 10 s. (**B**) Quantification of fluorescent signals for active CaMKII in each condition (n=50 for each). *$P<0.001$, Dunnett T3 test. (**C**, **D**) Inhibition of CaMKII activity by ant-AIP-II (a cell-permeable inhibitory peptide specific for CaMKII, 50 μM) from 30 min after the conditioning K^+ treatment impaired the maintenance of sustained phosphorylation of CaMKII Thr286/287 at 2 h. Immunofluorescent images (C) and their quantification (D, n=40 for each) are shown. *$P<0.001$, Dunnett T3 test.

increase, the CaMKII activity was attenuated to the basal level (Figure 5A). Thus, both of the positive-feedback pathways were required for the maintenance of CaMKII activity.

To further clarify the role of each positive-feedback loop, the effect of altering the strength of each phosphorylation on the CaMKII activity was examined. Figure 5B shows the strength of CaMKII autophosphorylation and that of PDE1 phosphorylation required to maintain certain levels of CaMKII activity after the transient $[Ca^{2+}]_i$ stimulation. The rate (k_{cat}) of CaMKII autophosphorylation predominantly determined the CaMKII activity. Thus, the activity level of CaMKII seemed to mainly rely on the CaMKII autophosphorylation rather than PDE1 inhibition. Next, we examined the effect of varying k_{cat} of each phosphorylation on CaMKII activation in response to the transient $[Ca^{2+}]_i$ increase (Figure 5C and D). When the k_{cat} of CaMKII autophosphorylation was too high, CaMKII automatically shifted to a high-activity state with the basal $[Ca^{2+}]_i$ (Figure 5C). Therefore, the strength of Thr286/287 autophosphorylation must be kept within a limited range for the CaMKII activity to shift from a low state to a high state in response to a transient $[Ca^{2+}]_i$ change. Similarly, weakening or strengthening the PDE1 phosphorylation narrowed the range for Ca^{2+}-dependent state switching of the CaMKII activity (Figure 5D). Figure 5E shows the ratio of CaMKII activity before and 30 min after the transient $[Ca^{2+}]_i$ increase with various strengths of two positive-feedback loops. These results indicated that balancing the two positive-feedback pathways is critical for sustained CaMKII activation in response to a $[Ca^{2+}]_i$ increase.

To elucidate the role of PDE1 inhibition by CaMKII, we analyzed how the CaMKII activity affects the PP-1 activity through PDE1 phosphorylation. As the amount of active CaMKII increased, active PP-1 decreased in a manner depending on PDE1 phosphorylation by CaMKII (Figure 5F). The rate of PDE1 phosphorylation determined the working range within which a change of the CaMKII activity effectively influenced the PP-1 activity. Thus, PDE1 inhibition by CaMKII seemed to dynamically change signaling cascades from a dephosphorylation-dominant state to a phosphorylation-dominant state through alteration of the PP-1 activity.

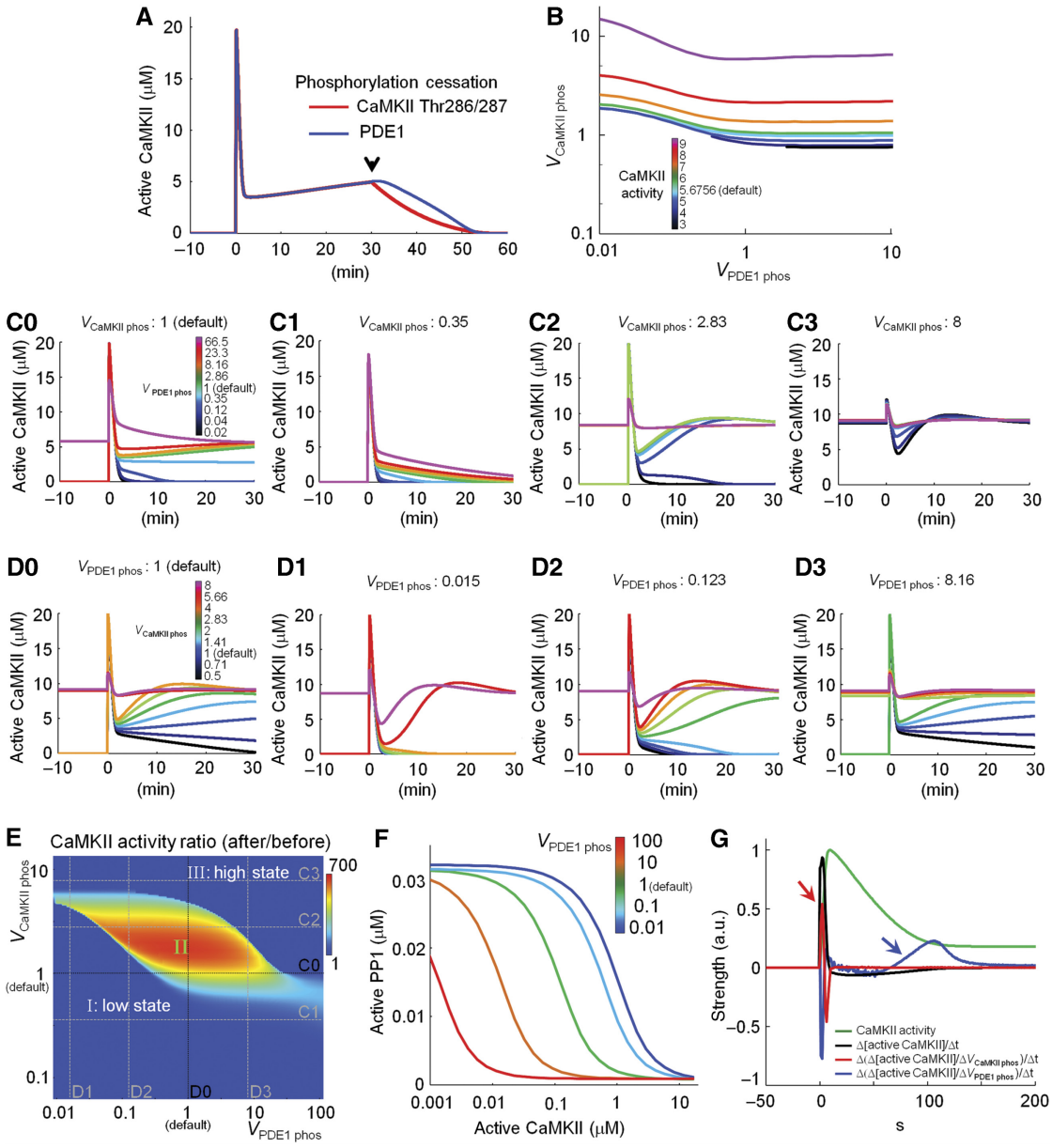

Figure 5 Bistability of signaling cascades depends on synergistic action of CaMKII autophosphorylation and PDE1 inhibition by CaMKII. (**A**) CaMKII autophosphorylation at Thr286/287 or PDE1 phosphorylation by CaMKII was stopped at 30 min after the conditioning $[Ca^{2+}]_i$ increase (1 μM for 10 s). Time courses of the amount of active CaMKII are shown. (**B**) The predominant role of CaMKII autophosphorylation in maintenance of the high CaMKII activity. The rate of CaMKII autophosphorylation at Thr286/287 (defined as the value relative to the default value: $V_{CaMKII\ phos}$) and that of PDE1 phosphorylation ($V_{PDE1\ phos}$) required to maintain the respective CaMKII activities in the steady state (presented with different colors). The CaMKII activity was predominantly determined by the strength of CaMKII autophosphorylation. (**C0-C3**, **D0-D3**) Time courses of the amount of active CaMKII before and after the transient $[Ca^{2+}]_i$ increase (1 μM for 10 s) with the indicated $V_{CaMKII\ phos}$ and $V_{PDE1\ phos}$. In C0-3, $V_{CaMKII\ phos}$ was fixed, whereas in D0-3, $V_{PDE\ phos}$ was fixed. (**E**) Heat map illustrating the CaMKII activity ratio before and 30 min after the transient $[Ca^{2+}]_i$ increase (1 μM for 10 s) as a function of $V_{CaMKII\ phos}$ and $V_{PDE1\ phos}$. Only in area II, the total CaMKII activity shifted from a low state to a high state on the conditioning $[Ca^{2+}]_i$ increase. In area I, the positive-feedback loops were too weak to sustain the high CaMKII activity. By contrast, in area III, the positive-feedback loops were so strong that CaMKII activity was in a high state in the basal condition. (**F**) Change of PP-1 activity by CaMKII-mediated PDE1 phosphorylation. The total amount of active CaMKII was altered in the model, and the resultant change of PP-1 activity was examined. The amount of active PP-1 was plotted against the amount of active CaMKII with various $V_{PDE1\ phos}$. (**G**) Time courses of the normalized CaMKII activity, the rate of change of the CaMKII activity, the rate of change of the CaMKII activity difference caused by slight alteration of $V_{CaMKII\ phos}$ or $V_{PDE1\ phos}$. Arrows indicate peaks of the activation of each positive-feedback loop.

Finally, we analyzed when each positive-feedback loop was influential in supporting the sustained CaMKII activation. The effectiveness of each positive-feedback loop was estimated by the CaMKII activity change brought about by 1% change of each k_{cat}. The effect of autophosphorylation at Thr286/287 on CaMKII activation peaked rapidly during the $[Ca^{2+}]_i$ increase, whereas that of PDE1 inhibition became stronger about 100 s after the $[Ca^{2+}]_i$ increase (Figure 5G; Supplementary Figure 4), when the decrease of CaMKII activity was suppressed. Thus, CaMKII autophosphorylation seems to augment the CaMKII activity soon

after the $[Ca^{2+}]_i$ increase, whereas the PDE1 inhibition pathway seems to attenuate the CaMKII inactivation later, presumably through suppressing the PP-1 activity.

Prediction of the model: role of PDE1 in the $[Ca^{2+}]_i$ threshold regulation

Using the simulation model, we next attempted to address how the threshold for RP induction is determined. There are two feedforward inhibitory pathways in the signaling network: one through calcineurin and the other through PDE1. These pathways might regulate the $[Ca^{2+}]_i$ threshold for RP induction. To examine this issue, we investigated how large an increase in $[Ca^{2+}]_i$ is required to induce sustained CaMKII activation by systematically altering the amplitude of transient $[Ca^{2+}]_i$ increase (from 0.1 to 1 μM for 10 s) with 0.05-μM steps in the simulation model. To establish a sustained CaMKII activation, a $[Ca^{2+}]_i$ increase larger than 0.6 μM was required (Figure 6A).

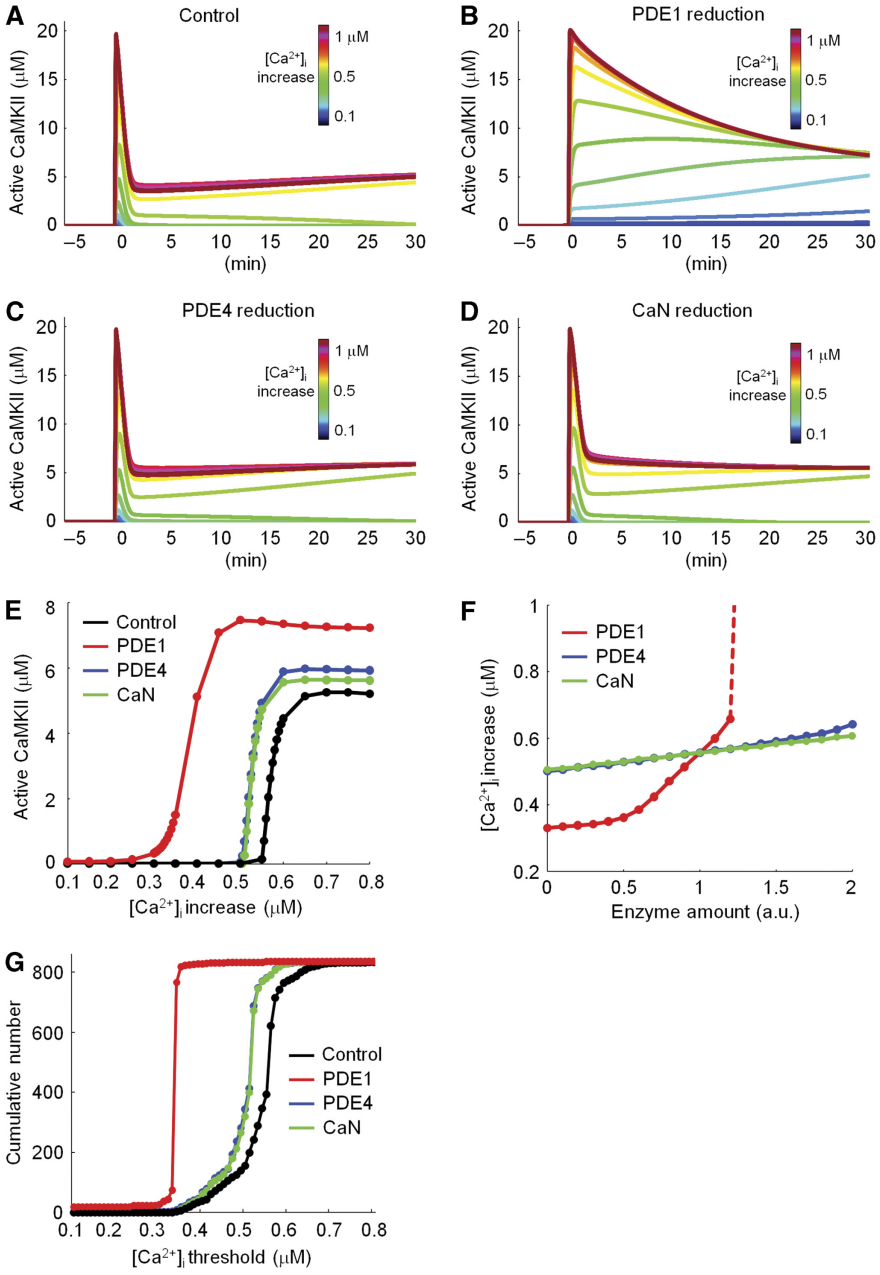

Figure 6 Simulation showing that PDE1 determines the $[Ca^{2+}]_i$ threshold for induction of sustained CaMKII activation. (**A**–**D**) Time courses of the amount of active CaMKII before and after various amplitudes of $[Ca^{2+}]_i$ increase for 10 s without (A) or with 80% reduction of the amount of PDE1 (B), PDE4 (C), or calcineurin (CaN, D). (**E**) The amount of active CaMKII 30 min after the $[Ca^{2+}]_i$ increase in each condition was plotted against the amplitude of $[Ca^{2+}]_i$ increase. (**F**) The amplitude of the $[Ca^{2+}]_i$ increase required for the sustained CaMKII activation (>1 μM at 30 min) was plotted against the amount of each enzyme (value relative to the default value). (**G**) Robustness of the predominant role of PDE1 in the Ca^{2+} threshold regulation. Cumulative distributions of the Ca^{2+} thresholds for induction of sustained CaMKII activation. The 843 different parameter sets were examined with or without an 80% decrease of PDE1, PDE4, or CaN. Source data is available for this figure at www.nature.com/msb.

Next, we examined the impact of the PDE1-mediated feedforward inhibitory pathway on the $[Ca^{2+}]_i$ threshold. When the concentration of PDE1 was reduced to 20% in the model, an increase of $[Ca^{2+}]_i$ to 0.35 μM triggered sustained CaMKII activation (Figure 6B). The reduction of PDE1 caused a leftward shift of the concentration–response curve for CaMKII activation by a transient $[Ca^{2+}]_i$ increase (Figure 6E). Thus, the $[Ca^{2+}]_i$ threshold required for the sustained CaMKII activation was markedly lowered by PDE1 reduction. As the amount of PDE1 increased, the amplitude of $[Ca^{2+}]_i$ increase required for sustained CaMKII activation became larger (Figure 6F). In the absence of PDE1, the $[Ca^{2+}]_i$ increase required for triggering sustained CaMKII activation (>1 μM at 30 min) was 0.33 μM. On the other hand, a PDE1 increase of >30% made it impossible for any increase of $[Ca^{2+}]_i$ (up to 10 μM) to trigger sustained CaMKII activation. Thus, the amplitude of $[Ca^{2+}]_i$ increase required for sustained CaMKII activation was dynamically controlled by PDE1. In contrast, when the concentration of Ca^{2+}-independent PDE4 was altered, the $[Ca^{2+}]_i$ threshold required for sustained CaMKII activation was little affected (Figure 6C, E, and F). Thus, Ca^{2+}/CaM-dependent PDE1, but not Ca^{2+}/CaM-independent PDE4, raises the $[Ca^{2+}]_i$ threshold for long-term activation of CaMKII.

Next, we examined how the calcineurin-mediated feedforward inhibition affected the $[Ca^{2+}]_i$ threshold for sustained CaMKII activation. Surprisingly, alteration of the concentration of calcineurin had little effect on the $[Ca^{2+}]_i$ threshold (Figure 6D–F). Taken together, these results showed that, of the two feedforward inhibitory pathways, the PDE1 pathway rather than the calcineurin pathway predominantly determines the $[Ca^{2+}]_i$ threshold for induction of sustained CaMKII activation. The predominant role of PDE1 in controlling the $[Ca^{2+}]_i$ threshold was evident, even if the duration of $[Ca^{2+}]_i$ stimulation was shortened (Supplementary Figure 5).

As our kinetic simulation model contains multiple parameters (130 parameters in total except for $[Ca^{2+}]_i$: 19 for molecular concentrations, 76 for binding-dissociation reactions, and 35 for enzymatic reactions), it is critical to test whether the model prediction is robust to variations of parameters. To address this issue, we altered each parameter to 10 different values between 1/100 and 100 times of the default value (1/100, 1/50, 1/10, 1/5, 1/2, 2, 5, 10, 50, or 100), and examined the amplitude of $[Ca^{2+}]_i$ increase required to cause sustained CaMKII activation (>5% of total CaMKII at 30 min). Out of 1300 cases, 843 cases yielded Ca^{2+} threshold values that triggered sustained CaMKII activation (see Supplementary information). In the other 457 cases, the Ca^{2+} threshold could not be calculated, because of CaMKII activation with the basal $[Ca^{2+}]_i$ (107 cases), or because of the failure to trigger sustained CaMKII activation by a transient Ca^{2+} increase (0.1–2 μM) (350 cases). The Ca^{2+} threshold in the former 843 cases (65% of total) was 0.54 ± 0.08 μM (mean ± s.d.), which was close to the value of the original model (0.56 μM). When GABA increase (100 μM) was coupled with the threshold $[Ca^{2+}]_i$ increase, the CaMKII activation was markedly suppressed in all cases (2 ± 7% activity of that without GABA increase, mean ± s.d.). Thus, CaMKII was persistently activated by the transient $[Ca^{2+}]_i$ increase and suppressed by the coupled $GABA_BR$ activation in many cases, even if the value of each parameter varied widely, suggesting the robustness of our model's scheme.

Next, we analyzed how the Ca^{2+} thresholds calculated in the 843 cases with different parameter sets were affected by reducing the amount of PDE1, calcineurin, or PDE4 (see Supplementary information). Although reduction of PDE4 or calcineurin to 20% of the default amount had little effect on the Ca^{2+} threshold (PDE4, 0.50 ± 0.08 μM; calcineurin, 0.50 ± 0.07 μM), the PDE1 reduction markedly decreased the Ca^{2+} threshold to induce sustained CaMKII activation in most cases (0.34 ± 0.08 μM). Interestingly, the cumulative distribution of Ca^{2+} thresholds calculated from 3372 cases in total (Figure 6G) resembled the relationship between the amplitude of $[Ca^{2+}]$ increase and the CaMKII activity at 30 min after the $[Ca^{2+}]$ increase in the original model (see Figure 6E). Thus, a predominant role of PDE1 in controlling the Ca^{2+} threshold was not specific to the default model setting but was inherent in the signaling cascades modeled here. Furthermore, the detailed sensitivity analysis of the model evaluating the impact of each parameter on the Ca^{2+} threshold suggested that the feedforward inhibitory pathway of CaMKII consisting of Ca^{2+}/CaM, PDE1, cAMP, PKA, DARPP-32, and PP-1 had a significant influence on the Ca^{2+} threshold (see Supplementary information). Taken together, these results indicate that PDE1 predominantly and robustly determined the Ca^{2+} threshold for sustained CaMKII activation in the model.

Verification of PDE1-mediated control of the $[Ca^{2+}]_i$ threshold for RP induction

If the theoretical predictions could be confirmed by experiments, the validity of the model would be strongly supported. Thus, we attempted to experimentally test the prediction that PDE1 has a predominant function in the $[Ca^{2+}]_i$ threshold for RP induction. First, we searched for conditions to increase $[Ca^{2+}]_i$ to different levels in cultured Purkinje neurons using $[Ca^{2+}]_i$ imaging combined with whole-cell patch-clamp recording. We recorded the $[Ca^{2+}]_i$ increase in response to the conditioning stimulation consisting of five depolarization pulses (0 mV at 0.5 Hz) with five different durations (20, 40, 60, 100, or 500 ms). To measure $[Ca^{2+}]_i$ effectively in the range in which we were interested (200–600 nM), we loaded two fluorescent Ca^{2+} indicator dyes with different dissociation constants, fura-2 (50 μM, K_d=144 nM) and fura-4F (50 μM, K_d=770 nM, a derivative of fura-2) into a Purkinje neuron through a glass patch pipette. The conditioning stimulation with 20, 40, 60, 100, and 500 ms pulses increased the fluorescence ratio (F340/F380) to 0.67 ± 0.05, 0.73 ± 0.06, 0.94 ± 0.11, 1.59 ± 0.28, and 3.07 ± 0.46, respectively, in the proximal dendrites of a Purkinje neuron (Figure 7A and B). These values corresponded to $[Ca^{2+}]_i$ of about 0.13, 0.16, 0.25, 0.45, and 2 μM, respectively.

Using these conditioning stimulations, we examined the $[Ca^{2+}]_i$ threshold for RP induction. RP was monitored by measuring the amplitude of current response to GABA iontophoretically applied to the proximal dendrites of a Purkinje neuron under a voltage-clamp condition (at −70 mV). Strong conditioning stimulation consisting of depolarization pulses for 500 ms potentiated the amplitude

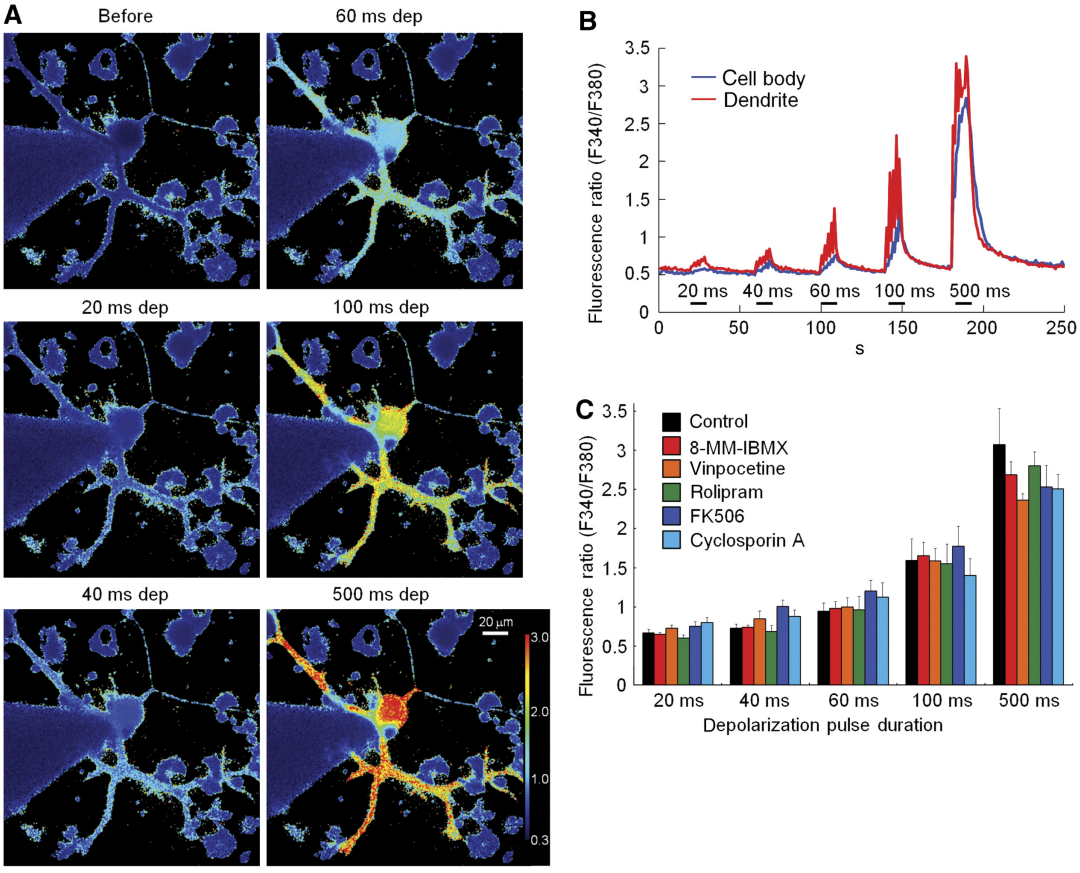

Figure 7 The $[Ca^{2+}]_i$ increases caused by five different patterns of conditioning stimulation. (**A**) Representative fluorescence ratio images (F340/F380) before and after five depolarizing pulses (0 mV at 0.5 Hz) with duration of 20, 40, 60, 100, or 500 ms. (**B**) Averaged time courses of fluorescence ratio from eight Purkinje neurons in the soma and proximal dendrites before and after the conditioning stimulations. (**C**) Effects of 8-MM-IBMX (20 μM), vinpocetine (100 μM), rolipram (10 μM), FK506 (300 nM), or cyclosporine A (5 μM) on the $[Ca^{2+}]_i$ increase in the proximal dendrite of a Purkinje neuron. *n*=8 for each. No significant difference was detected between the control and other groups (two-way ANOVA). Source data is available for this figure at www.nature.com/msb.

of the current response to GABA for >30 min (176 ± 13% at 30 min, mean ± s.e.m), and this potentiation was impaired by inhibition of either CaMKII (93 ± 4%) by a specific inhibitor peptide AIP-II (1 μM) or PKA (95 ± 4%) by KT5720 (10 μM) (Figure 8A). Thus, we confirmed our earlier observation that RP is induced by a large $[Ca^{2+}]_i$ increase depending on the CaMKII and PKA activities. Next, we examined the threshold for RP induction. As shown in Figure 8B, conditioning stimulation consisting of shorter depolarization pulses than 500 ms failed to induce RP (500 ms, 175 ± 21%; 100 ms, 110 ± 18%; 60 ms, 100 ± 13%; 40 ms, 109 ± 2%; 20 ms, 108 ± 17%). Taken together, the findings show that RP was induced in an all-or-none manner dependent on the $[Ca^{2+}]_i$ increase (at least >0.45 μM for 10 s).

Next, we examined whether the $[Ca^{2+}]_i$ threshold was controlled by PDE1. When PDE1 was inhibited by 8-MM-IBMX, conditioning stimulation consisting of 40-ms depolarization pulses was sufficient to induce RP (500 ms, 174 ± 7%; 100 ms, 172 ± 28%; 60 ms, 177 ± 2%; 40 ms, 173 ± 15%; 20 ms, 99 ± 6%) (Figure 8C). Another PDE1 inhibitor, vinpocetine (100 μM), also lowered the threshold for RP induction (500 ms, 165 ± 14%; 100 ms, 171 ± 12%; 60 ms, 169 ± 22%; 40 ms, 161 ± 14%; 20 ms, 102 ± 3%) (Figure 8D). PDE1 inhibition did not significantly affect the $[Ca^{2+}]_i$ increase triggered by each conditioning depolarization (Figure 7C) or the basal $GABA_AR$ responsiveness (Supplementary Table 1). Interestingly, RP caused by weak conditioning stimulations (40- or 60-ms depolarization pulses) developed slowly after the conditioning and finally reached a level similar to that caused by a strong conditioning stimulation, which resembled the time course of simulated CaMKII activation (see Figure 6B). Taken together, these results indicate that PDE1 inhibition substantially lowered the $[Ca^{2+}]_i$ required for RP induction, as predicted by the simulation, indicating a critical role of PDE1 in the $[Ca^{2+}]_i$ threshold control.

On the other hand, inhibition of PDE4 by a specific inhibitor, rolipram (10 μM), did not affect the threshold for the RP induction (500 ms, 168 ± 6%; 100 ms, 105 ± 9%; 60 ms, 109 ± 3%; 40 ms, 100 ± 9%; 20 ms, 108 ± 20%) (Figure 8E). Inhibition of PDE4 by rolipram affected neither the extent of $[Ca^{2+}]_i$ increase in response to each conditioning stimulation (Figure 7C) nor the basal $GABA_AR$ responsiveness (Supplementary Table 1). Thus, PDE4 has a marginal role in the regulation of the $[Ca^{2+}]_i$ threshold for RP induction.

Finally, we examined the effect of the calcineurin-mediated feedforward inhibitory pathway on the threshold for RP induction. When calcineurin was inhibited by an inhibitor, FK506 (300 nM), the conditioning stimulation consisting of

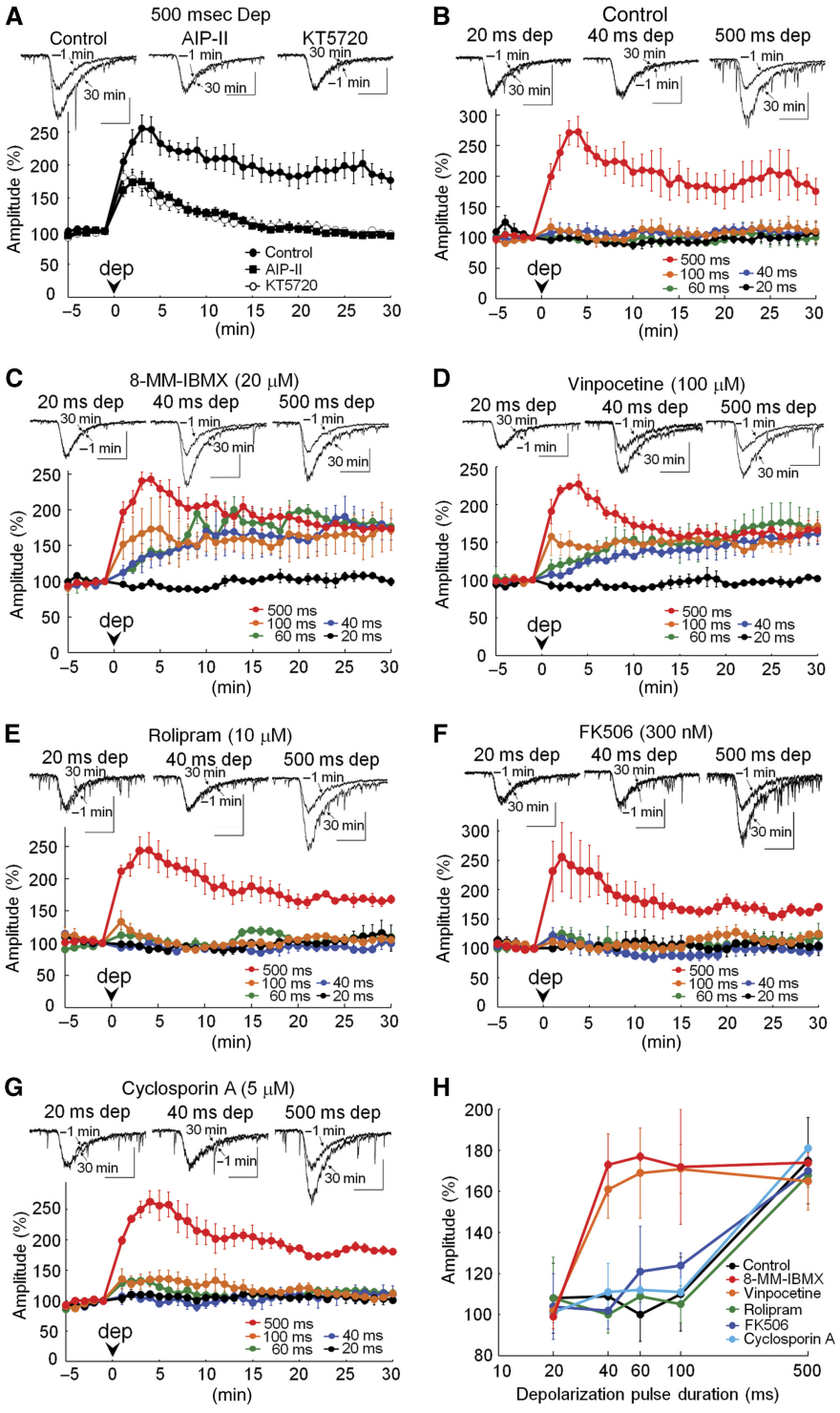

Figure 8 PDE1 predominantly regulates the threshold for RP induction. (**A**) Time courses of amplitude of GABA currents and representative current traces before and after the conditioning depolarization (0 mV for 500 ms, five times at 0.5 Hz) in the absence (control), or presence of AIP-II or KT5720. n=5 for each. (**B**–**G**) Time courses of amplitude of GABA currents before and after conditioning stimulation consisting of five depolarization pulses with duration of 20, 40, 60, 100, or 500 ms in the absence (B, control) or presence of 8-MM-IBMX (C), vinpocetine (D), rolipram (E), FK506 (F), or cyclosporine A (G). n=3 for each. Representative current traces before and 30 min after the conditioning stimulation composed of five depolarization pulses with duration of 20, 40, or 500 ms are also shown in each panel. Scale bars indicate 200 pA and 1 s. (**H**) The relationship between the strength of conditioning stimulation (duration of each depolarization pulse) and the extent of GABA response potentiation at 30 min. PDE1 inhibition by either 8-MM-IBMX or vinpocetine significantly lowered the threshold for RP induction compared with the control ($P<0.001$, two-way ANOVA, and Dunnet T3 test).

500-ms depolarization pulses, but not of shorter pulses induced RP (500 ms, 170 ± 7%; 100 ms, 124 ± 6%; 60 ms, 121 ± 22%; 40 ms, 102 ± 9%; 20 ms, 104 ± 16%) (Figure 8F). These values were similar to those in the control condition. Likewise, another inhibitor, cyclosporin A (5 μM), did not affect the threshold for RP induction (500 ms, 181 ± 2%; 100 ms, 111 ± 7%; 60 ms, 112 ± 2%; 40 ms, 111 ± 14%; 20 ms, 101 ± 5%) (Figure 8G). Neither FK506 nor cyclosporine A significantly affected the extent of $[Ca^{2+}]_i$ increase during the conditioning stimulation (Figure 7C) or the basal $GABA_AR$ responsiveness (Supplementary Table 1). These results support the idea that calcineurin-mediated feedforward inhibition is not significantly involved in the control of the $[Ca^{2+}]_i$ threshold.

As summarized in Figure 8H, inhibition of PDE1, but not of PDE4 or calcineurin, significantly lowered the threshold for RP induction. Thus, PDE1 is a critical regulator of the $[Ca^{2+}]_i$ threshold for RP induction so that RP is not induced by a weak stimulation.

Discussion

We developed a kinetic simulation model for signaling cascades regulating inhibitory synaptic plasticity in cerebellar Purkinje neurons. The computational simulation showed that a transient $[Ca^{2+}]_i$ increase induced long-term activation of CaMKII, which was suppressed by $GABA_BR$ activation coupled with the $[Ca^{2+}]_i$ increase. Thus, our simulation model reproduced the switching of CaMKII activity in response to different patterns of neuronal activity, closely corresponding to RP induction and its suppression (Kawaguchi and Hirano, 2000, 2002). Our model showed that synergistic action of two positive-feedback reactions, the CaMKII autophosphorylation at Thr286/287 and the negative regulation of PDE1 by CaMKII, is critical for the sustained CaMKII activation. Furthermore, the simulation analysis suggested that Ca^{2+}/CaM-activated PDE1 raised the $[Ca^{2+}]_i$ threshold for RP induction. This theoretical prediction was confirmed by electrophysiological experiments showing that inhibition of PDE1, but not that of PDE4 or calcineurin, markedly lowered the $[Ca^{2+}]_i$ threshold for RP induction. Thus, the combined applications of computational simulation and cell biological experiments revealed a critical role of the feedforward inhibition of CaMKII by PDE1 in regulating the threshold for RP induction.

Molecular networks that maintain synaptic plasticity

The long-term maintenance of synaptic plasticity is likely to rely on the persistent modification of the amount or activity of certain molecules caused by a transient neuronal activity. A positive-feedback loop in molecular networks is a candidate mechanism to enable the sustained modification. Experimental and simulation studies have suggested that autophosphorylation of CaMKII Thr286/287 works as a key positive-feedback loop for the long-term synaptic plasticity (Bhalla and Iyengar, 1999; Lisman *et al*, 2002; Hayer and Bhalla, 2005; Miller *et al*, 2005; Sanhueza *et al*, 2007; Urakubo *et al*, 2008). In this study, we also showed that autophosphorylation is critical for the persistent CaMKII activation. However, when the k_{cat} of CaMKII autophosphorylation was too high, the CaMKII activity automatically shifted to a high state even in the basal condition (see Figure 5). The strength of the positive-feedback loop also depends on the affinity of CaMKII for Ca^{2+}/CaM, as the autophosphorylation at Thr286/287 occurs after the association. Considering that β-CaMKII has 10-fold higher affinity for Ca^{2+}/CaM than α-CaMKII, the ratio of α- and β-isoforms expressed in Purkinje neurons might be critical for the strength of the positive-feedback loop. Indeed, alteration of the affinity of CaMKII and Ca^{2+}/CaM significantly affected the Ca^{2+}-mediated CaMKII activation (see Supplementary information).

In addition, we showed that the CaMKII-mediated reduction of PDE1 affinity with Ca^{2+}/CaM forms another positive-feedback loop. The PKA activity seems to be regulated by the activity of PDE1 in the basal condition owing to the high affinity of PDE1 for Ca^{2+}/CaM (K_d ∼0.1 nM) (Meyer *et al*, 1992). Indeed, a reduction of PDE1 activity increased cAMP, facilitating the PKA activity and DARPP-32 phosphorylation. As a result, PP-1 was inhibited by phospho-DARPP-32 (see Figures 2 and 5). Thus, the positive-feedback loop consisting of PDE1 inhibition by CaMKII shifted the molecular network from a dephosphorylation-dominant state to a phosphorylation-dominant state through suppressing PP-1 activity. The synergistic action of CaMKII autophosphorylation at Thr286/287 and PDE1 inhibition by CaMKII underlies the state switching of molecular networks regulating RP.

A positive-feedback loop consisting of MAPK (mitogen-activated protein kinase) and PKC (protein kinase C) has also been suggested to contribute to synaptic plasticity at excitatory synapses (Bhalla and Iyengar, 1999; Kuroda *et al*, 2001; Tanaka and Augustine, 2008). MAPK and PKC activate each other indirectly through PLA_2, arachidonic acid, and Raf (Bhalla *et al*, 2002), contributing to sustained CaMKII activation through PKC-mediated up-regulation of a type of adenylyl cyclase (Bhalla and Iyengar, 1999).

How the sustained CaMKII activation potentiates the responsiveness of $GABA_AR$s to establish RP remains to be clarified. CaMKII augments the activity of $GABA_AR$ through phosphorylating the β and γ subunits (Houston and Smart, 2006; Houston *et al*, 2008). Considering that $GABA_AR$s in Purkinje neurons are composed of α1, β2/3, and γ2 subunits (Laurie *et al*, 1992), CaMKII-mediated up-regulation of $GABA_AR$ might directly contribute to the expression of RP. We recently reported that a CaMKII-mediated sustained conformational change of $GABA_AR$-associated protein (GABARAP), which directly binds to $GABA_AR$ γ2 subunits, is critical for the induction and maintenance of RP (Kawaguchi and Hirano, 2007). Thus, RP might be induced by CaMKII through sustained phosphorylation of $GABA_AR$s and modulation of GABARAP.

Regulation of the threshold for RP induction by PDE1

Regulation of the threshold for synaptic plasticity has been suggested to correlate with learning ability (Migaud *et al*, 1998; Tang *et al*, 1999; Takeuchi *et al*, 2008). Although RP

induction is triggered by a $[Ca^{2+}]_i$ increase, how large an increase in $[Ca^{2+}]_i$ is required for inducing RP, and what kind of molecules determine the $[Ca^{2+}]_i$ threshold have hitherto remained unknown. This study clarified that Ca^{2+}/CaM-activated PDE1 constitutes a feedforward inhibitory pathway and controls the $[Ca^{2+}]_i$ threshold by suppressing the CaMKII activity through cAMP, PKA, DARPP-32, and PP-1. In contrast, calcineurin activation by Ca^{2+}/CaM, another feedforward inhibitory pathway, has little effect on the $[Ca^{2+}]_i$ threshold. This difference in the involvement of PDE1 and calcineurin in the threshold regulation might arise from the different time courses of their effects on the PP-1 activity. PDE1 causes weaker but longer-lasting DARPP-32 dephosphorylation indirectly through alteration of the PKA activity (see Supplementary Figure 6). Thus, PP-1 activation caused by the PDE1 pathway peaks tens of seconds after the end of the $[Ca^{2+}]_i$ increase, when the sustained CaMKII activation is established. The limited influence of calcineurin activity on the Ca^{2+} threshold for RP induction is presumably attributable to its shorter-lasting effect on PP-1 activity and the lower affinity for Ca^{2+}/CaM compared with PDE1.

Although calcineurin was not significantly involved in the Ca^{2+} threshold for RP induction, it is critical for the $GABA_BR$-mediated suppression of RP induction (Kawaguchi and Hirano, 2002). In the RP suppression, strong CaMKII autophosphorylation at Thr286/287 caused by the large $[Ca^{2+}]_i$ increase seems to be counteracted by potent activation of PP-1 synergistically brought about by the calcineurin activity triggered by the $[Ca^{2+}]_i$ increase and the $GABA_BR$-mediated downregulation of adenylyl cyclase activity.

To our knowledge, this is the first clarification that PDE1 has an important function in regulating the $[Ca^{2+}]_i$ threshold for synaptic plasticity. PDE1 is widely expressed in the central nervous system (Polli and Kincaid, 1994; Yu *et al*, 1997). Thus, the PDE1-mediated feedforward inhibition of CaMKII and the positive-feedback loop consisting of CaMKII-mediated PDE1 inhibition might underlie regulation of the threshold and/or the maintenance of many forms of synaptic plasticity. LTP-inducing high-frequency stimulation has been reported to cause sustained DARPP-32 phosphorylation by PKA in a manner dependent on CaMKII in hippocampal slices (Atkins *et al*, 2005). It was also reported that mutant mice lacking PDE1B show deficits in spatial learning (Reed *et al*, 2002).

Regulatory mechanism of RP and its functional relevance

RP is heterosynaptically induced by excitatory synaptic inputs such as those from a climbing fiber (Kano *et al*, 1992), whereas it is suppressed by activation of a presynaptic inhibitory interneuron (Kawaguchi and Hirano, 2000). Recently, we reported that mGluR1 activity supports RP induction by facilitating the PKA/phospho-DARPP-32/PP-1 inhibition pathway (Sugiyama *et al*, 2008). A cell-adhesion molecule, integrin, a receptor for extracellular matrix proteins, also negatively regulates RP induction through the Src-family of protein tyrosine kinases (Kawaguchi and Hirano, 2006). Thus, RP induction might be regulated through spatio-temporally integrating multiple synaptic inputs from inhibitory interneurons, a climbing fiber, and parallel fibers, and signals arising from cell-adhesion molecules.

Here, we have shown that the amplitude rather than the duration of $[Ca^{2+}]_i$ increase is critical for triggering sustained CaMKII activation, and that longer duration of the $[Ca^{2+}]_i$ increase only slightly lowers the amplitude of $[Ca^{2+}]_i$ threshold (see Figure 3), suggesting that RP might be induced by temporally integrating the $[Ca^{2+}]_i$ signal with a substantial leak. On the other hand, the suppression of sustained CaMKII activation largely depended on the duration of $GABA_BR$ activation. Thus, RP seems to be induced by high-frequency excitatory inputs within a limited period and suppressed by tonic inhibitory inputs.

RP at inhibitory synapses and LTD at excitatory synapses on a Purkinje neuron, which has been regarded as a cellular basis for motor learning, seem to correlate in many respects. The leaky integration of $[Ca^{2+}]_i$ signals for inducing plasticity noted above was also reported in LTD (Tanaka *et al*, 2007). Several molecules involved in RP, such as CaMKII, mGluR1, and Src, are also involved in LTD (Ito, 2001; Hansel *et al*, 2001, 2006; Tsuruno *et al*, 2008). Thus, the induction of both RP and LTD might be regulated interdependently. It was proposed that the increase in cGMP caused by nitric oxide gates the MAPK-PKC positive-feedback loop, which is critical for LTD induction (Ito, 2001; Ogasawara *et al*, 2007). Considering that PDE1 also hydrolyzes cGMP, PDE1 might also contribute to the gating of the MAPK-PKC positive-feedback loop and the LTD induction. Thus, RP at inhibitory synapses might contribute to refined information processing in the cerebellar cortex in concert with LTD at excitatory synapses.

Materials and methods

Construction of simulation model

A computational model of signaling cascades regulating RP induction was constructed incorporating our earlier results (Kawaguchi and Hirano, 2000, 2002), with some modifications (Figure 1). In Purkinje neurons, unlike hippocampal CA1 pyramidal neurons, Ca^{2+}/CaM-activated adenylyl cyclases such as type-1 and type-8 are not expressed (Cooper *et al*, 1995). Thus, in the model we assumed a certain activity level of G_s-type trimeric G protein, which activates adenylyl cyclase. G_s-coupled receptors such as dopamine receptors, serotonin receptors, and metabotropic glutamate receptors are expressed in Purkinje neurons (Schweighofer *et al*, 2004; Sugiyama *et al*, 2008). We also added PDE to the model. At least two types of PDE that degrade cAMP are expressed in Purkinje neurons. One is Ca^{2+}/CaM-activated PDE1, which breaks down both cAMP and cGMP (Polli and Kincaid, 1994). The other is cAMP-specific PDE4 (Cherry and Davis, 1999). Thus, cAMP produced by adenylyl cyclase was broken down by these PDEs in the model. The affinity of a type of PDE1 (PDE1B) to Ca^{2+}/CaM is reduced to one sixth by CaMKII-mediated phosphorylation (Hashimoto *et al*, 1989). PDE1B is highly expressed in Purkinje neurons (Yu *et al*, 1997). Thus, CaMKII-mediated inhibition of PDE1 was incorporated into the model. It produces a positive-feedback loop in the molecular network, because PDE1 inhibition increases the intracellular cAMP concentration, thus promoting the PKA activity, which in turn supports the CaMKII activity through inhibition of PP-1 by phospho-DARPP-32. Additionally, autophosphorylation of CaMKII at Thr286 in the α-isoform and at Thr287 in the β-isoform renders the enzyme Ca^{2+}-independently active (Miller and Kennedy, 1986; Lisman *et al*, 2002). Thus, CaMKII autophosphorylation at Thr286/287 also functions as a positive-feedback loop. Both the α- and β-isoforms of CaMKII are expressed in Purkinje neurons (see Supplementary Figure 1). Compared with α-type, β-CaMKII has about 10-fold higher affinity for Ca^{2+}/CaM. Thus, the ratio of α- and β-types

is critical for the sensitivity of CaMKII to a $[Ca^{2+}]_i$ increase. Here, the model was constructed assuming that equal amounts of α- and q β-subtypes are expressed in Purkinje neurons (see Supplementary information).

Biochemical reactions in the signaling cascades were represented either as binding-dissociation reactions or enzymatic reactions. For example, a binding reaction in which A and B bind to form complex AB is expressed as the following equation:

$$A + B \underset{k_b}{\overset{k_f}{\rightleftarrows}} AB, \quad (1)$$

where k_f and k_b are the rate constants for the forward and backward processes. These rate constants are determined by the dissociation constant K_d and time constant τ. K_d is defined as k_b/k_f, and τ reflects velocity of the reaction toward equilibrium. The reaction is represented as a differential equation:

$$\frac{d[AB]}{dt} = k_f[A][B] - k_b[AB]. \quad (2)$$

The enzymatic reaction was expressed with the Michaelis–Menten formulation:

$$S + E \underset{k-1}{\overset{k_1}{\rightleftarrows}} SE \xrightarrow{k_{cat}} P + E, \quad (3)$$

where S, E, and P are substrate, enzyme, and product, respectively. The Michaelis constant K_m is defined as $K_m=(k_{-1}+k_{cat})/k_1$. The maximum enzyme velocity V_{max} is expressed as $V_{max}=k_{cat}\cdot[E]_{total}$, where $[E]_{total}$ is the total concentration. Details of the model construction, kinetic reactions, and parameters are presented in the Supplementary information.

We performed the simulation using GENESIS software with kinetikit interface (Bhalla and Iyengar, 1999). Ordinary differential equations were numerically solved by the exponential Euler method with a time step of 1 ms except for a certain period around stimulation. The integration time step was set at 0.01 ms for 200 s after the onset of stimulation to minimize the calculation error. We started simulation experiments after the model reached equilibrium in the basal condition.

Culture

The method for preparing primary cultures of cerebellar neurons was similar to that in an earlier study (Kawaguchi and Hirano, 2006). Whole-cell patch-clamp recordings and immunocytochemistry were performed 3 weeks after preparation of the culture. Experimental procedures were performed in accordance with the guidelines regarding care and use of animals for experimental procedures of the National Institutes of Health, USA, and Kyoto University, and approved by the local committee for handling experimental animals in the Graduate School of Science, Kyoto University.

Electrophysiology

Methods used for electrophysiological experiments were similar to those in earlier studies (Kawaguchi and Hirano, 2000, 2002). Briefly, whole-cell patch-clamp recording from a cerebellar Purkinje neuron grown in culture for 3 weeks was performed with an amplifier (EPC9, HEKA) in a solution containing (in mM) 145 NaCl, 5 KOH, 2 $CaCl_2$, 1 $MgCl_2$, 10 Hepes, and 10 glucose (pH 7.3) at room temperature (20–24°C). The solution contained 6-cyano-7-nitroquinoxaline-2, 3-dione disodium (CNQX, 10 μM, Tocris Cookson, UK), tetrodotoxin (TTX, 1 μM, Wako, Japan), and SCH50911 (10 μM, Tocris Cookson) to inhibit glutamatergic EPSCs, action potentials, and $GABA_BR$ activation, respectively. Purkinje neurons were visually identified by their large cell body and thick dendrites. A patch pipette used to record from a Purkinje neuron was filled with an internal solution (pH 7.3, adjusted by CsOH) containing (in mM) 121 CsCl, 33 KCl, 1.4 ethylene glycol bis (β-aminoethylether) *N*,*N*,*N*′,*N*′-tetraacetic acid (EGTA), 10 Hepes, 2 Mg-ATP, and 0.2 Na-GTP. Mg-ATP and Na-GTP were used to minimize rundown of $GABA_AR$. The membrane potential of a Purkinje neuron was held at −70 mV. Only recordings with input resistance of >100 MΩ and series resistance of <25 MΩ were accepted. To minimize the voltage-clamp error, the amplitude of GABA response at the beginning of experiments was set at around 200 pA. Series resistance and input resistance were monitored every 2 min and experiments were terminated when a change of >20% was detected. The method for iontophoretic application of GABA was similar to that in earlier studies (Kawaguchi and Hirano, 2000, 2002, 2006, 2007). A glass pipette containing 10 mM GABA was aimed at a proximal dendrite, and 20-ms positive voltage pulses were applied every 20 s. 8-MM-IBMX (20 μM, Calbiochem, USA), cyclosporine A (5 μM, Tocris Cookson), rolipram (10 μM, Biomol International, USA), or KT5720 (10 mM, Calbiochem) was applied to the bath 5–10 min before recording. FK506 (300 nM, Calbiochem), vinpocetine (100 μM, Biomol International), or AIP-II (1 μM, Calbiochem) was applied intracellularly through a patch pipette. On the basis of the K_i or IC50 values for each pharmacological agent (8-MM-IBMX, 5–10 μM; vinpocetine, 10–20 μM; rolipram, 1–2 μM; FK506, 1–100 nM; cyclosporine A, 10–200 nM) (Némoz *et al*, 1989; Bram *et al*, 1993; Yu *et al*, 1997), we estimated that the activity of each enzyme was inhibited by about 80–90%.

Immunocytochemistry

Cultured neurons were fixed with 4% paraformaldehyde in phosphate buffered saline, permeabilized with 0.5% Tween 20, then blocked with 2% skim milk or 4% goat serum (Sigma, USA), and finally labeled with primary and secondary antibodies. The following antibodies were used: a mouse monoclonal antibody (mAb) against calbindin D28 (1:500, Swant Bellinzona, Switzerland), a mAb against α-CaMKII (1:500, Chemicon, USA), a mAb against β-CaMKII (1:500, Zymed Laboratories, Inc., USA), a rabbit polyclonal antibody (pAb) against active CaMKII (1:500, Promega, USA), a rabbit pAb against PDE1B (1:200, Chemicon, USA), a rabbit pAb against PDE4 (1:100, Santa Cruz Biotechnol. Inc., USA), a rabbit pAb against MAP2 (1:1000, Santa Cruz Biotechnol. Inc.), and Alexa 568- or Alexa 488-conjugated pAb against rabbit or mouse IgG (1:400, Molecular Probes, USA). Fluorescent images were recorded with a confocal laser microscope (FV1000 imaging system, Olympus, Japan), and analyzed using IP lab software (Solution Systems, Japan). The high K^+-containing conditioning treatment solution was prepared by replacing 50 mM Na^+ with K^+ in the normal external solution. After the conditioning treatment of cultured cerebellar neurons for 10 s, neurons were washed with the normal external solution, and then returned to the culture medium until fixation. A cell-permeable inhibitory peptide of CaMKII (Ant-AIP-II, 50 μM, Calbiochem) or KN62 (5 μM, Calbiochem) was added to the culture medium 30 min after the conditioning treatment with the high K^+ solution. The averaged fluorescent signals for active CaMKII in the area positive for calbindin, a molecular marker of Purkinje neurons, were compared.

Ca^{2+} imaging

$[Ca^{2+}]_i$ was measured with a Ca^{2+} imaging system (Aquacosmos, Hamamatsu Photonics, Japan) mounted on an upright microscope (BX50WI, Olympus) using fura-2 and fura-4F (50 μM each, Invitrogen, USA). These dyes were loaded into a Purkinje neuron through a patch pipette, and excited alternately at 340 and 380 nm for 120 ms. Each fluorescence image was recorded at 1 Hz, and the fluorescence ratio (the fluorescence excited at 340 nm divided by that at 380 nm) was calculated. As shown in Supplementary Figure 7, fitting of the *in vitro* calibration data on our imaging system provided the following equation for conversion of the ratio values into $[Ca^{2+}]_i$ values (nM):

$$[Ca^{2+}]_i = 550\times\left(\frac{\text{ratio}-R_{min}}{R_{max}-\text{ratio}}\right)^{\frac{1}{1.6}}, \quad (4)$$

where R_{max} and R_{min} are the maximum and minimum values of the fluorescence ratio. R_{max} (3.35) was determined by averaging five values obtained by *in vivo* calibration, in which 5 μM ionomycin was applied to Purkinje neurons in the presence of 2 mM Ca^{2+} in the extracellular solution. R_{min} (0.39) was obtained by applying 15 mM Cs-BAPTA to a Purkinje neuron.

Statistics

Data are presented as mean ± s.e.m. unless otherwise stated. Statistical significance was assessed by one-way or two-way ANOVA followed by the *post hoc* Dunnet T3 test, unless otherwise stated.

Supplementary information

Supplementary information is available at the *Molecular Systems Biology* website (www.nature.com/msb).

Acknowledgements

We are grateful to Drs Shinya Kuroda and Hidetoshi Urakubo for their valuable suggestions and advice, and to Drs Elizabeth Nakajima and Yoshiaki Tagawa for helpful comments on the manuscript. This work was supported by grants from the Ministry of Education, Culture, Sports, Science, and Technology, Japan to SK and TH, and from the Uehara Memorial Foundation to SK, and by Global COE program A06 of MEXT, Japan, to Kyoto University.

Conflict of interest

The authors declare that they have no conflict of interest.

References

Atkins CM, Davare MA, Oh MC, Derkach V, Soderling TR (2005) Bidirectional regulation of cytoplasmic polyadenylation element-binding protein phosphorylation by Ca^{2+}/calmodulin-dependent protein kinase II and protein phosphatase 1 during hippocampal long-term potentiation. *J Neurosci* **25:** 5604–5610

Bailey CH, Giustetto M, Huang YY, Hawkins RD, Kandel ER (2000) Is heterosynaptic modulation essential for stabilizing Hebbian plasticity and memory? *Nat Rev Neurosci* **1:** 11–20

Bhalla US, Iyengar R (1999) Emergent properties of networks of biological signaling pathways. *Science* **283:** 381–387

Bhalla US, Ram PT, Iyengar R (2002) MAP kinase phosphatase as a locus of flexibility in a mitogen-activated protein kinase signaling network. *Science* **297:** 1018–1023

Bram RJ, Hung DT, Martin PK, Schreiber SL, Crabtree GR (1993) Identification of the immunophilins capable of mediating inhibition of signal transduction by cyclosporin A and FK506: roles of calcineurin binding and cellular location. *Mol Cell Biol* **13:** 4760–4769

Brandman O, Meyer T (2008) Feedback loops shape cellular signals in space and time. *Science* **322:** 390–395

Cherry JA, Davis RL (1999) Cyclic AMP phosphodiesterases are localized in regions of the mouse brain associated with reinforcement, movement, and affect. *J Comp Neurol* **407:** 287–301

Cooper DM, Mons N, Karpen JW (1995) Adenylyl cyclases and the interaction between calcium and cAMP signalling. *Nature* **374:** 421–424

Doi T, Kuroda S, Michikawa T, Kawato M (2005) Inositol,1,4,5-trisphosphate-dependent Ca^{2+} threshold dynamics detect spike timing in cerebellar Purkinje cells. *J Neurosci* **25:** 950–961

Gaiarsa JL, Caillard O, Ben-Ari Y (2002) Long-term plasticity at GABAergic and glycinergic synapses: mechanisms and functional significance. *Trends Neurosci* **25:** 564–570

Hansel C, de Jeu M, Belmeguenai A, Houtman SH, Buitendijk GH, Andreev D, De Zeeuw CI, Elgersma Y (2006) αCaMKII is essential for cerebellar LTD and motor learning. *Neuron* **51:** 835–843

Hansel C, Linden DJ, D'Angelo E (2001) Beyond parallel fiber LTD: the diversity of synaptic and non-synaptic plasticity in the cerebellum. *Nat Neurosci* **4:** 467–475

Hashimoto Y, Sharma RK, Soderling TR (1989) Regulation of Ca^{2+}/calmodulin- dependent cyclic nucleotide phosphodiesterase by the autophosphorylated form of Ca^{2+}/calmodulin-dependent protein kinase II. *J Biol Chem* **264:** 10884–10887

Hayer A, Bhalla US (2005) Molecular switches at the synapse emerge from receptor and kinase traffic. *PLoS Comput Biol* **1:** 137–154

Houston CM, Hosie AM, Smart TG (2008) Distinct regulation of β2 and β3 subunit-containing cerebellar synaptic $GABA_A$ receptors by calcium/calmodulin-dependent protein kinase II. *J Neurosci* **28:** 7574–7584

Houston CM, Smart TG (2006) CaMK-II modulation of $GABA_A$ receptors expressed in HEK293, NG108-15 and rat cerebellar granule neurons. *Eur J Neurosci* **24:** 2504–2514

Ito M (2001) Cerebellar long-term depression: characterization, signal transduction, and functional roles. *Physiol Rev* **81:** 1143–1195

Kandel ER (2001) The molecular biology of memory storage: a dialogue between genes and synapses. *Science* **294:** 1030–1038

Kano M, Kano M, Fukunaga K, Konnerth A (1996) Ca^{2+}-induced rebound potentiation of γ-aminobutyric acid-mediated currents requires activation of Ca^{2+}/calmodulin-dependent kinase II. *Proc Natl Acad Sci USA* **93:** 13351–13356

Kano M, Rexhausen U, Dreessen J, Konnerth A (1992) Synaptic excitation produces a long-lasting rebound potentiation of inhibitory synaptic signals in cerebellar Purkinje cells. *Nature* **356:** 601–604

Kawaguchi S, Hirano T (2000) Suppression of inhibitory synaptic potentiation by presynaptic activity through postsynaptic $GABA_B$ receptors in a Purkinje neuron. *Neuron* **27:** 339–347

Kawaguchi S, Hirano T (2002) Signaling cascade regulating long-term potentiation of $GABA_A$ receptor responsiveness in cerebellar Purkinje neurons. *J Neurosci* **22:** 3969–3976

Kawaguchi S, Hirano T (2006) Integrin α3β1 suppresses long-term potentiation at inhibitory synapses on the cerebellar Purkinje neuron. *Mol Cell Neurosci* **31:** 416–426

Kawaguchi S, Hirano T (2007) Sustained structural change of $GABA_A$ receptor-associated protein underlies long-term potentiation at inhibitory synapses on a cerebellar Purkinje neuron. *J Neurosci* **27:** 6788–6799

Komatsu Y (1996) $GABA_B$ receptors, monoamine receptors, and postsynaptic inositol trisphosphate-induced Ca^{2+} release are involved in the induction of long-term potentiation at visual cortical inhibitory synapses. *J Neurosci* **16:** 6342–6352

Kuroda S, Schweighofer N, Kawato M (2001) Exploration of signal transduction pathways in cerebellar long-term depression by kinetic simulation. *J Neurosci* **21:** 5693–5702

Laurie DJ, Seeburg PH, Wisden W (1992) The distribution of 13 $GABA_A$ receptor subunit mRNAs in the rat brain. II. Olfactory bulb and cerebellum. *J Neurosci* **12:** 1063–1076

Lisman J, Schulman H, Cline H (2002) The molecular basis of CaMKII function in synaptic and behavioural memory. *Nat Rev Neurosci* **3:** 175–190

Malenka RC, Nicoll RA (1999) Long-term potentiation-a decade of progress? *Science* **285:** 1870–1874

Meyer T, Hanson PI, Stryer L, Schulman H (1992) Calmodulin trapping by calcium-calmodulin-dependent protein kinase. *Science* **256:** 1199–1202

Migaud M, Charlesworth P, Dempster M, Webster LC, Watabe AM, Makhinson M, He Y, Ramsay MF, Morris RG, Morrison JH, O'Dell TJ, Grant SG (1998) Enhanced long-term potentiation and impaired learning in mice with mutant postsynaptic density-95 protein. *Nature* **396:** 433–439

Miller SG, Kennedy MB (1986) Regulation of brain type II Ca^{2+}/calmodulin-dependent protein kinase by autophosphorylation: a Ca^{2+}-triggered molecular switch. *Cell* **44:** 861–870

Miller P, Zhabotinsky AM, Lisman JE, Wang XJ (2005) The stability of a stochastic CaMKII switch: dependence on the number of enzyme molecules and protein turnover. *PLoS Biol* **3:** e107

Némoz G, Moueqqit M, Prigent AF, Pacheco H (1989) Isolation of similar rolipram-inhibitable cyclic-AMP-specific

phosphodiesterases from rat brain and heart. *Eur J Biochem* **184:** 511–520

Nusser Z, Hajos N, Somogyi P, Mody I (1998) Increased number of synaptic $GABA_A$ receptors underlies potentiation at hippocampal inhibitory synapses. *Nature* **395:** 172–177

Ogasawara H, Doi T, Doya K, Kawato M (2007) Nitric oxide regulates input specificity of long-term depression and context dependence of cerebellar learning. *PLoS Comput Biol* **3:** e179

Pettigrew DB, Smolen P, Baxter DA, Byrne JH (2005) Dynamic properties of regulatory motifs associated with induction of three temporal domains of memory in *Aplysia*. *J Comput Neurosci* **18:** 163–181

Polli JW, Kincaid RL (1994) Expression of a calmodulin-dependent phosphodiesterase isoform (PDE1B1) correlates with brain regions having extensive dopaminergic innervation. *J Neurosci* **14:** 1251–1261

Reed TM, Repaske DR, Snyder GL, Greengard P, Vorhees CV (2002) Phosphodiesterase 1B knock-out mice exhibit exaggerated locomotor hyperactivity and DARPP-32 phosphorylation in response to dopamine agonists and display impaired spatial learning. *J Neurosci* **22:** 5188–5197

Sanhueza M, McIntyre CC, Lisman JE (2007) Reversal of synaptic memory by Ca^{2+}/calmodulin-dependent protein kinase II inhibitor. *J Neurosci* **27:** 5190–5199

Schweighofer N, Doya K, Kuroda S (2004) Cerebellar aminergic neuromodulation: towards a functional understanding. *Brain Res Brain Res Rev* **44:** 103–116

Sheng M, Kim MJ (2002) Postsynaptic signaling and plasticity mechanisms. *Science* **298:** 776–780

Sugiyama Y, Kawaguchi S, Hirano T (2008) mGluR1-mediated facilitation of long-term potentiation at inhibitory synapses on a cerebellar Purkinje neuron. *Eur J Neurosci* **27:** 884–896

Takeuchi T, Ohtsuki G, Yoshida T, Fukaya M, Wainai T, Yamashita M, Yamazaki Y, Mori H, Sakimura K, Kawamoto S, Watanabe M, Hirano T, Mishina M (2008) Enhancement of both long-term depression induction and optokinetic response adaptation in mice lacking delphilin. *PLoS ONE* **3:** e2297

Tanaka K, Augustine GJ (2008) A positive feedback signal transduction loop determines timing of cerebellar long-term depression. *Neuron* **59:** 608–620

Tanaka K, Khiroug L, Santamaria F, Doi T, Ogasawara H, Ellis-Davies GC, Kawato M, Augustine GJ (2007) Ca^{2+} requirements for cerebellar long-term synaptic depression: role for a postsynaptic leaky integrator. *Neuron* **54:** 787–800

Tang YP, Shimizu E, Dube GR, Rampon C, Kerchner GA, Zhuo M, Liu G, Tsien JZ (1999) Genetic enhancement of learning and memory in mice. *Nature* **401:** 63–69

Tsuruno S, Kawaguchi SY, Hirano T (2008) Src-family protein tyrosine kinase negatively regulates cerebellar long-term depression. *Neurosci Res* **61:** 329–332

Urakubo H, Honda M, Froemke RC, Kuroda S (2008) Requirement of an allosteric kinetics of NMDA receptors for spike timing-dependent plasticity. *J Neurosci* **28:** 3310–3323

Yu J, Wolda SL, Frazier AL, Florio VA, Martins TJ, Snyder PB, Harris EA, McCaw KN, Farrell CA, Steiner B, Bentley JK, Beavo JA, Ferguson K, Gelinas R (1997) Identification and characterisation of a human calmodulin-stimulated phosphodiesterase PDE1B1. *Cell Signal* **9:** 519–529